PHILOSOPHICAL TRANSACTIONS OF THE ROYAL SOCIETY A MATHEMATICAL, PHYSICAL & ENGINEERING SCIENCES

Crustal Shortening in the Zambezi Belt [and Discussion]

M. W. C. Barr and C. J. Talbot

Phil. Trans. R. Soc. Lond. A 1976 **280**, 555-567
doi: 10.1098/rsta.1976.0013

Phil. Trans. R. Soc. Lond. A. **280**, 555–567 (1976) [555]
Printed in Great Britain

Crustal shortening in the Zambezi Belt

By M. W. C. Barr
Hunting Geology and Geophysics, Elstree Way, Boreham Wood, Herts., U.K.

Pan-African deformation in the Zambezi Belt appears to be dominated by the development of domes and periclines cored by gneiss, whose growth has swept aside the overlying meta-sediments and constricted them in synclinoria which tend to be disposed tangentially about the main domal structures. Because of this arrangement, horizontal displacements tend to cancel out. By using strain data derived from pebbles in conglomerates which form part of the deformed sequence and by modelling the body rotations involved in this kind of tectonic pattern, shortening across part of the Belt in Zambia is estimated to be not more than 8 km or 14 %. The method is extended by using strain data from elsewhere in the Belt and by making further assumptions and extrapolations, to a section 230 km long extending to the northern margin of the Rhodesian Craton. Estimated shortening across this part of the Belt is unlikely to exceed 70 km or 25 %.

1. Introduction

Several papers elsewhere in this volume have illustrated the potential of palaeomagnetic studies in determining relative displacement of blocks of crust in the Proterozoic time interval. In this contribution an attempt is made to determine lateral displacement across a Proterozoic fold belt by using an alternative method, by removing the strains and distortions which have been observed in the folded rocks of the belt and adding together the displacements which these strains imply. In order to do this with any degree of precision, very detailed structural studies are required along the complete length of a section across the deformed zone. This probably cannot be achieved even for the most intensely studied belts, far less for the Zambezi Belt which is relatively little known and locally obscured by unfolded sedimentary rocks. For this reason, numerous assumptions and extrapolations have been made and the result may be seriously in error. Nevertheless, the broad agreement between the displacement derived here and estimates from palaeomagnetic evidence is encouraging, particularly since the methods are based on unrelated principles and use entirely different data.

The following notation is used in this article: X, Y, Z; labels attached to the principal semi-axes of an ellipsoid (the strain ellipsoid) derived by homogeneous deformation of a sphere of volume $\frac{4}{3}\pi$; of lengths $(1+e_1) \geqslant (1+e_2) \geqslant (1+e_3)$ respectively (Ramsay 1967, especially pp. 121–124). XY(F2); the principal plane containing the X and Y semi-axes of the strain ellipsoid representing deformation accompanying F2 folding. A similar notation is used for other lines or planes within strain ellipsoids representing the deformation of other, or combinations of several deformation episodes.

2. Geological setting

The structural setting of the area of discussion is shown in figure 1. The Zambezi Belt is a region of complex structure extending west from the Moçambique Belt and disappearing beneath the rocks of the Katanga fold belt in south-central Zambia and in the Kariba region

of Rhodesia. Its northern border is poorly defined but is thought locally to follow the line of the Mwembeshi Dislocation Zone (Drysdall, Johnson, Moore & Thieme 1972). Its southern limit follows the boundary between gneissic rocks characteristic of the northern escarpment zone of Rhodesia and the granites and greenstones typical of the cratonic nucleus of the country and has long been known from the work of Worst (1960), Workman (1961) and Wiles (1961). The pattern of radiometric ages is typical of Pan-African belts elsewhere in Africa and some of the structures continue into the Proterozoic Katanga fold belt in Zambia, but it is quite clear that, with the exception of the Umkondo System exposed principally in northeastern Rhodesia, most of the rocks have undergone polycyclic deformation and are much older than this in origin.

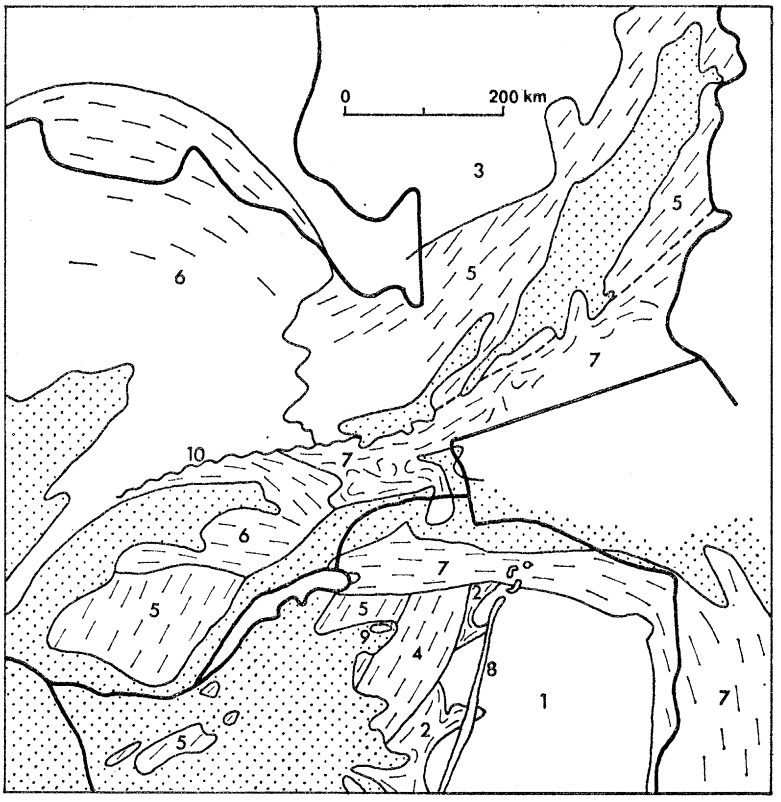

FIGURE 1. Structural setting of the area, largely after Vail (1968) and Drysdall *et al.* (1972). 1, Rhodesian Craton with 2, some greenstone belts shown. 3, Bangweulu Block. 4, Piriwiri–Lomagundi fold belt. 5, Irumide fold belt. 6, Katanga fold belt. 7, Moçambique and Zambezi Belts. 8, Great Dyke of Rhodesia. 9, Urungwe Klippe. 10, Mwembeshi Dislocation Zone. Stippled area, sedimentary cover.

The area of particular interest lies in the southeast corner of Zambia between 15° S and the Zambezi River and between 29° 30′ and 30° E. This part of the crust is typical of the belt in having been involved in several phases of deformation, metamorphism and granite and migmatite formation. The structure, outlined in figure 2, is dominated by domes and periclines separated by synclinoria which tend to lie tangential to the main domal structures and within which the metasedimentary rocks of the area are constricted. These structures are related to the Pan-African event which is also responsible for the main penetrative fabric in the rocks of the area. This deformation episode is labelled F2 and is superimposed on north–south isoclinal folds which belong to an earlier orogeny of unknown age, hereinafter labelled F1.

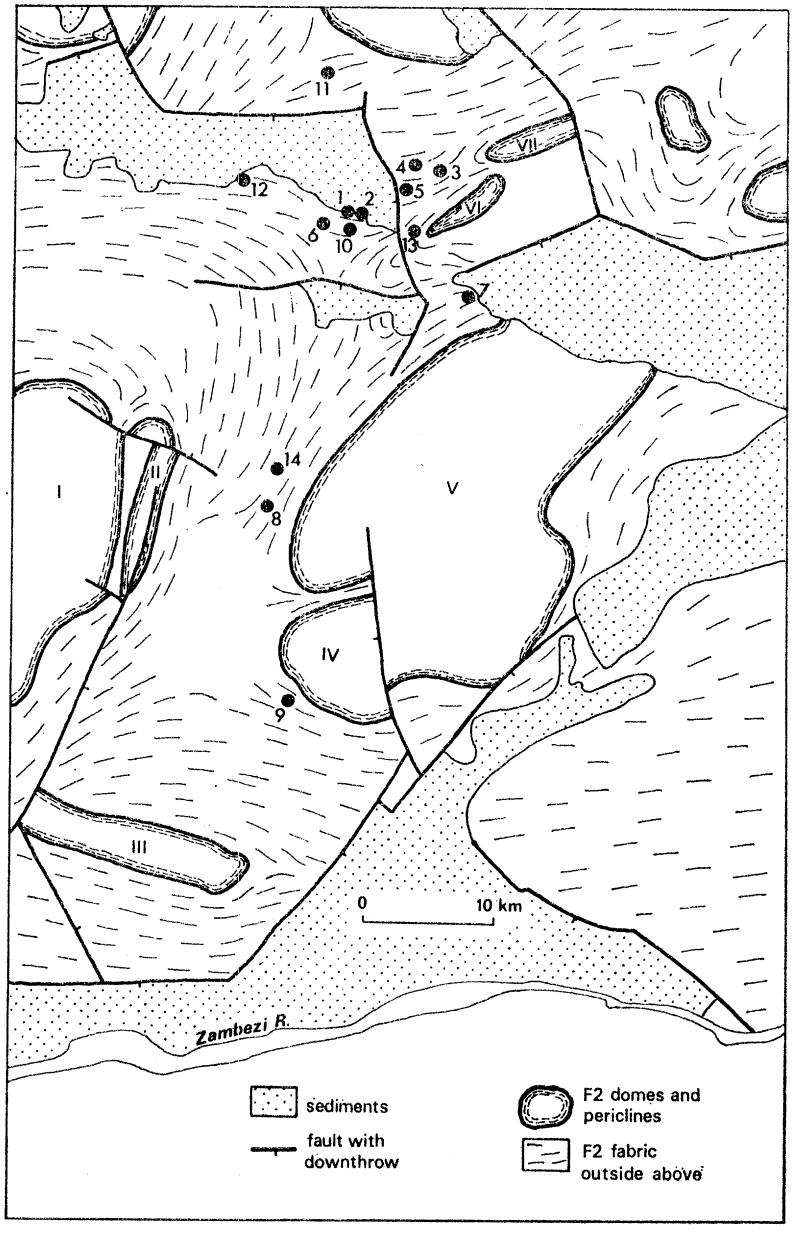

FIGURE 2. Structural outline of part of south-central Zambia. Filled circles, strain determination localities.

3. DATA

The main metamorphic sequence of the area has been involved in both the fold episodes mentioned above and several later ones. It consists of schists, quartzites and metavolcanic amphibolites with a well exposed and widespread series of deformed conglomerates within the topmost formation of the sequence, the Kangaluwe Formation.

The deformation undergone by the conglomerates was estimated by measuring pebble axial ratios and orientations at the localities shown in figure 2. The sample size, method of calculation and strain ratios at these localities are shown in table 1 and the state of strain in the deformed pebbles in figure 3.

Accepting for the time being the validity of this approach to estimating strains, the shape and orientation of the deformed conglomerate pebbles should reflect the total strain in the rocks, from which the components, due to Proterozoic deformation must be extracted. Fortunately, the later deformation episodes do not appear to affect the shape of the conglomerate pebbles and therefore the problem is simplified to one of separating that component of the total strain for which the main episode of Proterozoic deformation (F2) is responsible from those of earlier deformations and any contribution of sedimentary origin. While some progress has been made in this direction (Barr 1974, pp. 82–84) the available data are entirely inadequate for a complete resolution of the component strains at any locality; some approximations are clearly necessary.

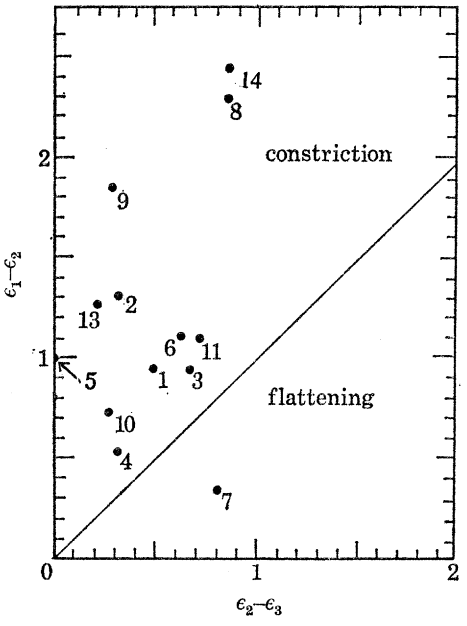

FIGURE 3. State of strain in deformed pebbles of the Kangaluwe Formation. $\epsilon_1-\epsilon_2 = \ln X/Y$; $\epsilon_2-\epsilon_3 = \ln Y/Z$

TABLE 1. STRAIN RATIOS DERIVED FROM DEFORMED PEBBLES IN CONGLOMERATES OF THE KANGALUWE FORMATION

	X/Y		Y/Z	
locality	method and no. of pebbles used†	value	method and no. of pebbles used†	value
1	A, 50	2.6	A, 50	1.6
2	A, 50	3.7	A, 50	1.35
3	B, 50	2.6	A, 50	1.9
4	B, 50	1.7	A, 50	1.35
5	B, 50	2.7	A, 94	1.0
6	B, 50	3.0	A, 50	1.85
7	B, 309	1.4	B, 309	2.3
8	B, 10	10.0	B, 10	2.4
9	B, 37	6.2	B, 37	1.3
10	B, 50	2.1	B, 50	1.3
11	visual estimate	3.0	visual estimate	2.0
12		n.d.	A, 79	1.8
13	B, 10	3.5	B, 17	1.2
14	B, 31	12.6	B, 59	2.3

† Methods; A, R_f/ϕ scatter diagram (Dunnet 1969); B, Geometric mean of pebble axial ratios.

At several exposures in the area, pebbles in the conglomerate have been buckled and folded with the banding around the hinge zones of F2 folds. At these exposures it can be seen that prior to F2 folding the long axes of the finite strain ellipsoid lay approximately in the banding. It has been assumed that this holds for most localities; this is likely considering the isoclinal style of F1 deformation. It follows that at those localities where the banding lies close in orientation to the XY plane of the total strain ellipsoid (all measurement localities except 5 and 9) the effect of the superimposition of F2 deformation has been to reinforce earlier strains, i.e. the values of the ratios Y/Z and X/Z are greater in the total strain ellipsoid than in that referred to either F1 or F2 deformation alone. The measured values are therefore the maximum possible for F2 strain.

One of the unusual features of the area is that the stretching direction of the rocks, defined by deformed amygdales and metamorphic spots as well as pebbles is everywhere sensibly parallel to F2 minor fold axes and the intersection of the banding with the F2 planar fabric. This implies one of the following combinations of conditions:

(*a*) stretching parallel to X(F2) was so great that all lines were rotated into approximate parallelism with X(F2).

(*b*) F2 folding had a controlling influence on the orientation of X(F2) which by chance everywhere lay parallel to one principal axis of the F1 strain ellipsoid; were the component strains superimposed in any way besides orthogonally then there should be a systematic difference in orientation between X(total strain) and linear elements of the F2 fabric.

(*c*) F2 folding had a controlling influence on the orientation of X(F2) and F1 deviatoric strain in sections containing X(total strain) was so small that it did not materially affect the orientation of the total strain ellipse.

Alternative (*a*) may be discounted since the total elongation at some exposures is small. Because of the extremely variable orientation of X(total strain) from place to place, it is extremely unlikely that alternative (*b*) accounts for the observed facts at many localities. It seems therefore that alternative (*c*) must apply. It follows that the elongation of the total strain ellipsoid at most exposures is the result of F2 deformation with only a small contribution from F1 strain and preferred pebble orientation of sedimentary origin. It is concluded that F2 strain ratios in sections containing X (total strain) probably closely approach and are unlikely to exceed the values for the total strain in these sections.

The conclusion of this brief discussion is that the use of total strain ratios in place of those referred to Proterozoic deformation sets a maximum limit on F2 strain. Now it became apparent early in this study that the shortening of the crust normal to the margins of the Zambezi Belt was unusually small. Therefore, in default of a more exact measurement of the displacement, impossible for reasons outlined above, it was considered that an estimate of the maximum amount of shortening would be the most interesting and instructive. It is apparent that the use of total strain ratios satisfies this limiting condition where the strain ellipsoid is orientated in such a way that lines normal to the margins of the Belt are shortened during Proterozoic deformation, but that it is necessary to determine *minimum* values for F2 strain ratios where the strain ellipsoid is orientated so as to stretch lines normal to the margins of the Belt. This applies to the centre and south of the area (south of D′, figure 4).

A very rough estimate of the F1 deviatoric strain in YZ sections of the total strain ellipsoid has been derived from exposures in the south of the area where the deformed pebbles are

PHILOSOPHICAL TRANSACTIONS OF THE ROYAL SOCIETY A MATHEMATICAL, PHYSICAL & ENGINEERING SCIENCES

buckled round the hinge zones of F2 folds. The estimate was made by using the geometric mean pebble axial ratio and assuming that the pebble sections in the fold limbs which lie with their long axes close to the axial planes of the F2 folds (taken to be XY(F2)) are about balanced by those in the hinge zones which make a large angle with them, so that the contribution of F2 deviatoric strain to the pebble ratio mean roughly cancels out. The estimated F1 ratio at these exposures is about 2.5:1. Here, as elsewhere, the long axes of the pebbles are parallel to F2 minor fold axes and the F1 contribution to the elongation cannot be estimated. It has been assumed therefore that the F1 strain ellipsoid is unlikely to fall in the constriction field since this seems to hold in most cleaved rocks (Ramsay & Wood 1973). The maximum estimated ratios for the F1 strain ellipsoid at these exposures are therefore $X:Y$, 2.5:1; $Y:Z$, 2.5:1.

Minimum values of F2 component ratios will be realized for given total strain ratios, where F1 and F2 strains are superimposed orthogonally with X(F2) $\parallel X$(F1), Y(F2) $\parallel Y$(F1) and Z(F2) $\parallel Z$(F1). These conditions are perhaps realized at localities 8 and 14 (figure 2), where the total strain ellipsoid lies with its long axes in the banding. Under these conditions X/Y(F2) $= \{X/Y$(total strain)$/X/Y$(F1)$\}$ and similarly for Y/Z(F2), resulting in X/Y(F2) ratios of 4:1, and 3.2:1 and Y/Z ratios of 1.05:1 and 1.09:1 at localities 8 and 14 respectively. The Y/Z ratios, which approach unity appear to be confirmed by the lack of any preferred orientation in the F2 planar fabric at these exposures. Ratios of $X:Y:Z$ of 3:1:1 will therefore be used as a minimum estimate of the F2 strain in conglomerates throughout the centre and south of the area.

In order to calculate displacements, it is necessary to know the orientation of the strain ellipsoid as well as the lengths of its semi-axes. The orientations used below were derived from the F2 strain trajectories determined by compiling F2 fabric data over much of the area of interest (Barr 1974, p. 64) and by assuming that planar elements of it, such as cleavage, schistosity and the axial planes of many minor folds are normal to the Z axis of the strain ellipsoid and that linear elements such as stretched pebbles, amygdales and metamorphic spots are parallel to the X axis (Barr 1974, pp. 74–76).

4. Method

The displacement of H′ relative to A (figure 4) was used as a measure of the average strain between the two localities. It was determined by computing the pre-F2 lengths and orientations of the rectilinear segments AB′, B′C′ . . . G′H′ in figure 4. This line was chosen because it lies reasonably close to localities where strain determinations have been made. Between A and D′ and line passes across the axis of a complex east–west synclinorium to which the F2 planar fabric is broadly axial planar. South of D′, the line trends close to the axis of a major F1 syncline which has been further tightened and elongated in a north–south direction during F2 deformation.

Each line segment in figure 4 was treated as if it were homogeneously strained. Ellipsoids representing this homogeneous strain were orientated parallel to the F2 strain trajectories in the vicinity of each line segment. Principal elongations were calculated assuming no volume change from the mean of strain determinations at nearby localities, except for segments south of D′ where ratios of $X:Y:Z$(F2) of 3:1:1 were used. The orientations and elongations used are shown in table 2.

The angles between each deformed line segment and the X, Y and Z axes of the relevant

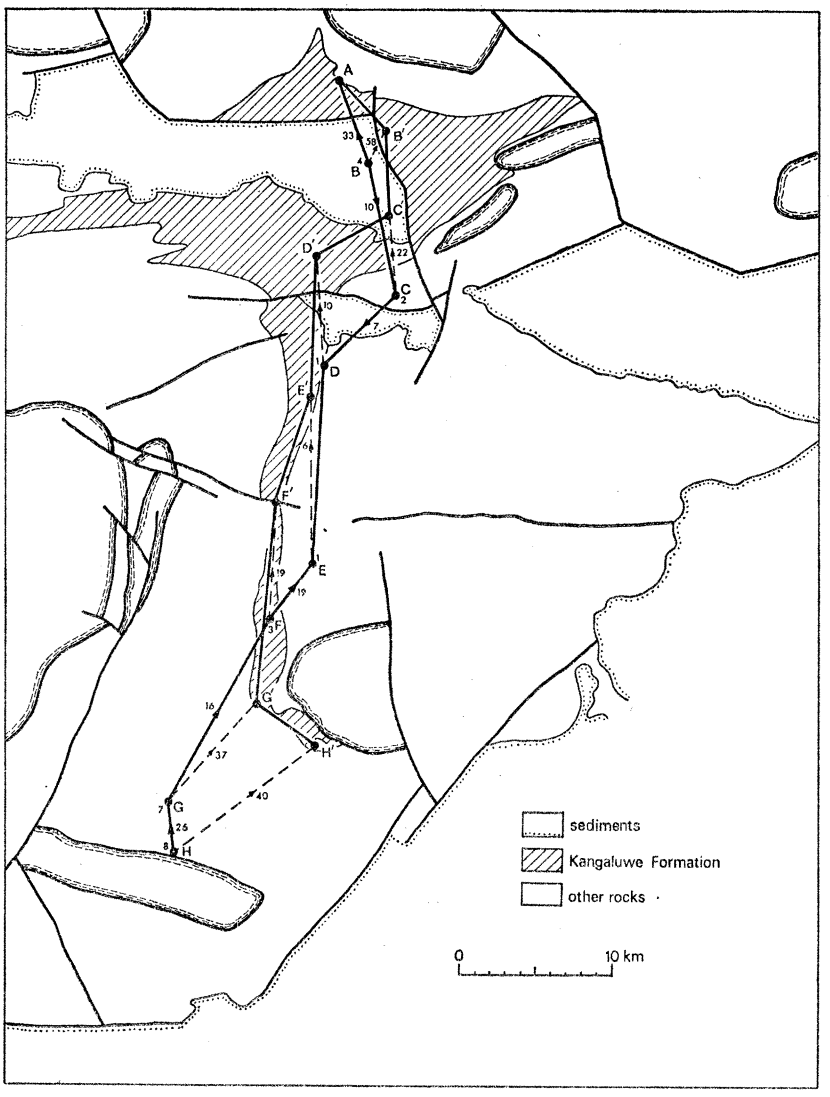

FIGURE 4. Relative displacements in the Rufunsa area during F2 deformation assuming irrotational strain. AB...H represents AB′...H′ in the undeformed state; numbers at B...H are the height of these stations in kilometres above A. Broken lines, plan projections of displacement vectors, sense of plunge and displacement and angle of plunge shown.

TABLE 2. PRINCIPAL AXIAL ORIENTATIONS AND PRINCIPAL ELONGATIONS USED IN DISPLACEMENT CALCULATIONS

	orientation, trend/plunge						
		F2 strain ellipsoid			elongations		
line segment	deformed line	X	Y	Z	$1+e_1$	$1+e_2$	$1+e_3$
AB′	318/0	113/35	229/30	348/41	2.62	0.87	0.44
B′C′	357/0	060/30	262/58	155/11	2.13	0.84	0.55
C′D′	241/0	110/63	251/21	348/15	2.58	0.85	0.46
D′E′	003/0	090/40	—	—	2.1	0.69	0.69
E′F′	017.5/0	180/15	—	—	2.1	0.69	0.69
F′G′	006/0	145/25	—	—	2.1	0.69	0.69
G′H′	310.5/0	145/25	—	—	2.1	0.69	0.69

PHILOSOPHICAL TRANSACTIONS OF THE ROYAL SOCIETY A MATHEMATICAL, PHYSICAL & ENGINEERING SCIENCES

strain ellipsoid (ϕ_1, ϕ_2 and ϕ_3 respectively), were measured stereographically and the reciprocal quadratic elongation along each line, λ^1, determined from the equation

$$\lambda' = \lambda_1' \cos^2 \phi_1 + \lambda_2' \cos^2 \phi_2 + \lambda_3' \cos^2 \phi_3 \quad \text{(Ramsay 1967, equations (4)–(7))}$$

where λ_1', λ_2', λ_3' are the reciprocal quadratic elongations along X, Y and Z respectively. The undeformed length of each line segment is given by (strained length)$(\lambda')^{\frac{1}{2}}$. The direction cosines of the undeformed lines were derived from the relation

$$\cos^2 \theta_1 = \cos^2 \phi_1 \lambda_1'/\lambda', \quad \cos^2 \theta_2 = \cos^2 \phi_2 \lambda_2'/\lambda', \quad \text{and} \quad \cos^2 \theta_3 = \cos^2 \phi_3 \lambda_3'/\lambda'$$

(derived from Ramsay 1967, equations (4–18)) where θ_1, θ_2 and θ_3, are the angles between the undeformed line and the X, Y and Z axes of the strain ellipsoid respectively. The trend and plunge of the undeformed lines were determined stereographically from θ_1, θ_2 and θ_3.

5. Results

The line which AB′...H′ represents before F2 deformation (assumed to be irrotational - see §6) is shown in figure 4 by AB...H. Numbers at B...H are their height in kilometres above A. Arrows and numbers show the sense and angle of plunge of each line segment. Also shown by broken lines are the plan projections of the displacement vectors B → B′, C → C′...H → H′ relative to A, with the sense of plunge and displacement, and the angle of plunge shown.

The displacement field which results comprises a north–south shortening in the east–west trending fold belt in the north of the area, and complementary north–south elongations in the centre and south of the area, which tend to cancel out. Material points in the centre of the east–west belt (e.g. B) have been displaced downwards relative to points towards its margin in agreement with the outcrop pattern. The displacement H → H′ relative to A is 13.5 km along a line plunging at 40° towards N 52° E. The mean longitudinal strain between A and H′ $(1+e)$ derived by comparing the lengths AH′ and AH is 0.84, corresponding to 16% shortening overall.

6. Discussion

These results illustrate the small displacements which are implied even in strongly deformed rocks where the orientation of the strain ellipsoid changes radically from place to place. However, they should be viewed in the light of possible sources of error. First, the strain which varies continuously in intensity and orientation along the line has been represented by a series of blocks and homogeneous strain with discontinuities at their interfaces. The result is therefore obviously imprecise. Secondly, the state of strain has been approximated so as to maximize northwards displacements relative to A; east–west and vertical components of displacement may therefore be considerably in error. Thirdly, only displacements reflected in the strained conglomerate pebbles have been taken into account; a major source of error therefore is displacements represented by strain discontinuities, such as F2 thrusts. By good fortune important F2 discontinuities are restricted to the north of the area and strike east–west with steep dip; any displacements which have taken place along them therefore will have relatively small north–south horizontal components. Fourthly, no account has been taken of body rotation during deformation; if the deformed material were free to rotate during straining then B (figure 4), for example, is not the unique location of B′ before deformation but is merely one

point on the surface of a sphere centred at A which describes all possible locations. The reasoning behind the rejection of extensive body rotation, which would seriously affect this displacement calculation is based on the F2 fabric pattern which appears to preclude large-scale body rotations at least about sub-vertical axes (Barr 1974, pp. 77–80). Ideally, it should be possible to estimate the rotations involved by reference to known features of the body of rock in the undeformed state, such as the orientation of planes and lines. Independent evidence suggests that F1 fold axes initially trended approximately north–south and had a low plunge. On this basis rotations should be applied during the 'unstraining' process south of F′ (figure 4) such that G and H are at about the same elevation as F and FG and GH are close to horizontal. This will only marginally increase the northwards component of the displacements H → H′. Similarly, opposite and approximately equal rotations about axes parallel to *X* are required between A and C to account for F2 folding in this region. This would increase the lengths of the segments AB and BC but will also change their orientation. The effect on the northwards component of the displacement C → C′ depends partly on the mechanism chosen to account for the folding and is probably small.

Finally, the whole calculation is based on the assumption that strains estimated at a few localities in one rock-type are representative of the state of strain along the complete length of the line AB′, B′C′...G′H′. All that can be said in justification is that pebbles in the conglomerates and deformed carbonate megacrysts in the Kangaluwe Formation schists at other localities along the line are not noticeably more eccentric than those measured at the strain determination localities.

TABLE 3. PERCENTAGE HORIZONTAL NORTH–SOUTH COMPONENTS OF DISPLACEMENT DERIVED FROM DEFORMED CONGLOMERATE PEBBLES IN THE KANGALUWE FORMATION

	percentage horizontal north–south component of displacement (+ elongation; − shortening)		
station	from A	between adjacent stations	from E
A	0		−35
		−39	
B	−39		−33
		−35	
C	−38		−33
		−45	
D	−39		−28
		−28	
E	−35		0
		+90	
F	−23		+90
		+7	
G	−14		+26
		−4	
H	−14		+21

I am inclined to accept therefore, that possible errors do not materially affect north–south components of displacement, amounting between A and H to 7.5 km over 54 km, or 14 % shortening (more detailed results are shown in table 3). These are maximum shortening figures; the actual value may be much smaller or may even be an elongation.

7. Extrapolation to a section across the Zambezi Belt

By combining the work of Talbot (1967) in the Chimanda area of Rhodesia with that presented in preceding sections and by making several further assumptions and extrapolations, it is possible to calculate the crustal shortening across the Zambezi Belt referred to Pan-African or Moçambiquian penetrative deformation. The main additional assumptions are that the intensity of F2 and post-Umkondo strain in the Rufunsa and Chimanda areas is typical of Moçambiquian deformation at intermediate localities, and that rotation during straining took place only about horizontal axes.

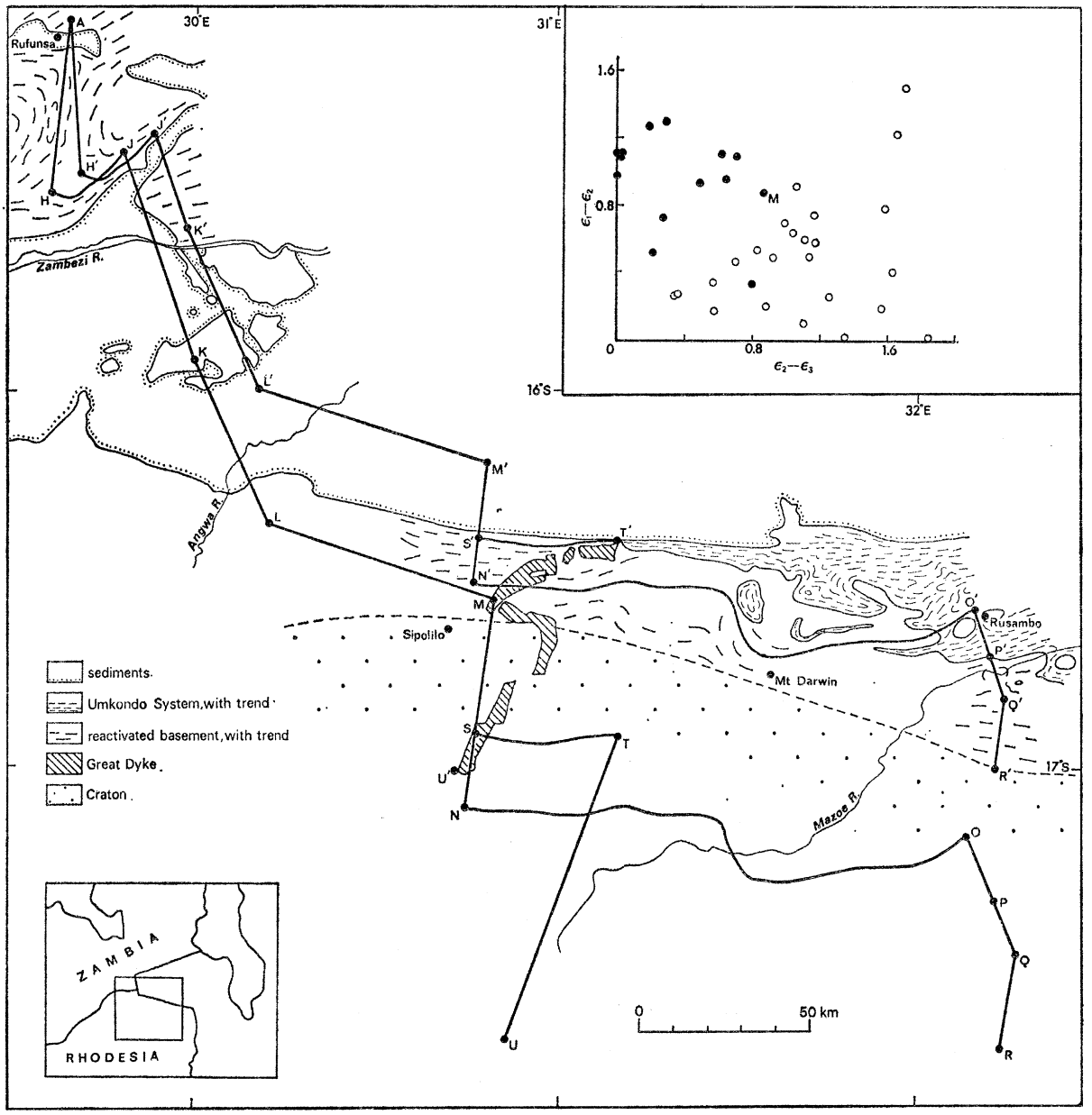

FIGURE 5. Crustal shortening across the Zambezi Belt. H...QR...TU represent the locations relative to A of H′...Q′R′...T′U′ before Zambezi Belt deformation. Inset: strain determinations in the Zambezi Belt; filled symbols, §3; open symbols, Talbot (1967).

The result of this calculation is presented in figure 5. The stations H...QR...TU represent locations relative to A of material points H′...Q′R′...T′U′ prior to Zambezi Belt deformation.

Directly applicable data are available only for segments AH′ (§3) and O′P′ (Talbot 1967, plate 2). The displacement P → P′ relative to O was calculated by constructing strain trajectories and calculating average principal elongations from Talbot's data. O′P′ was divided into segments, each of which was treated as if homogeneously strained. The orientation and location of the segments were dictated by the distribution of strain data and by the fact that heterogeneous body rotations which produced the fold culminations in the zone of linear trends and the gneiss domes in the zone of nodal trends took place about axes parallel to O′P′ (Talbot 1967) and therefore do not affect the calculated strain along it. The strain pattern in the Chimanda area proves to be quite similar to that of the Rufunsa area, with elongations about the gneiss domes tending to cancel shortening in the linear zone. However, the assumption of no volume strain in calculating principal elongations is probably invalid; strain ellipsoids in the pelitic rocks are distinctly more oblate that those in the other rock-types (see Ramsay & Wood 1973).

The shortening across P′Q′ is extrapolated from that across O′P′ and is justified by the similarity in the style of deformation in the country crossed by these lines (Talbot 1971, plate 1). The shortening across Q′R′ is a guess based on the possibility that it does not exceed that in the terrain immediately to the north. The line is drawn perpendicular to the regional foliation which dips west of south at about 45° (Swift 1959, unpublished map; R. M. Shackleton, private communication).

The magnitude of the strain undergone by segments J′K′ and M′N′ is a mean of the Rufunsa and the best Chimanda determinations (figure 5, inset). Plane strain was assumed for convenience and may well apply when large enough bodies of rock are considered. The orientation of the *XY* plane of the finite strain ellipsoid was taken to be parallel to planar elements of the F2 fabric for J′K′ and the dominant foliation (Vail 1966; Wiles 1968) for M′N′. *X* plunges down the dip of the F2 planar fabric at J′ and this orientation was assumed for the whole length of J′K′. According to Wiles (1968), slickensides (? quartz fibres) on boudins north of Sipolilo plunge down the dip of the foliation; this was assumed to be the orientation of *X*.

Segments H′J′, L′M′, N′O′, S′T′ are drawn parallel to the dominant foliation trace (Wagner 1913; Lightfoot 1923; Lightfoot & Tyndale-Biscoe 1931; Worst 1960; Vail 1965, 1966; Wiles 1968). Assuming

(*a*) that the foliation lies parallel to the *XY* plane of the finite strain ellipsoid;
(*b*) that the strain was plane on the scale of the line segments with *Y* horizontal;
(*c*) body rotation took place only about *Y*,

these segments are displaced but undistorted.

Segment K′L′ probably crosses granulites. If at all similar to the rocks of the southeast extremity of Zambia, K′L′ was virtually undeformed during the development of the Zambezi Belt. TU represents the arc length of the western margin of the Great Dyke between T′ and U′.

Since the *XY* plane of the strain ellipsoid (foliation) dips south across the strained segments, the latter plunged uniformly north before deformation assuming strictly irrotational deformation. The calculated vertical displacement R → R′ relative to A is −96 km, implying that A was initially some 96 km lower in elevation than R. Accepting that R′ is located within crustal material, A should be within the mantle. Since it is clearly nothing of the kind, irrotational deformation cannot apply. Body rotations have therefore been applied in undeforming all

segments such that the stations H...QR...TU are at the same elevation as H'...Q'R'...T'U'. Since the layering in the Great Dyke remains horizontal in the deformed zone (Worst 1960) this assumption is probably justified for segment M'N'.

8. Conclusions

The calculated north–south separation of A and R is 309 km and the northward component of the displacement R → R' relative to A is 73 km, corresponding to a shortening across the belt of just less than 25 % (figure 5). This compares with 25 % shortening calculated for the northern part of Talbot's area alone, and exceeds the 14 % calculated for the north and central parts of the Rufunsa area. The displacement is subject to numerous uncertainties; the precision limits on it are probably very much larger than the displacement itself.

The computed northward displacement of U relative to S compares closely with that of R relative to S, suggesting that the shortening across the belt at SU derived by assuming that the Great Dyke is buckle-folded in the Zambezi Belt, is closely comparable to the shortening at OR. However, the shortening across NS should be considerably greater than that shown if buckling of the dyke is assumed. This mechanism also implies some rotation about vertical axes in deforming NS.

In spite of the many shortcomings, this result is of interest because of the small displacement indicated which contrasts with that associated with plate motions and fold belt formation of Phanerozoic times. Moreover, as far as is known at the moment, the complete width of the Zambezi Belt is underlain by crust of continental type; there is no evidence that oceanic crust was involved in the formation of the fold belt and therefore no reason to believe that it formed part of an island arc system or lay at the margin of a Proterozoic continent.

References (Barr)

Barr, M. W. C. 1974 The pre-Karroo Geology of the Rufunsa Area, Zambia with special reference to structure and metamorphism. Unpublished Ph.D. thesis, University of Leeds.

Drysdall, A. R., Johnson, R. L., Moore, T. A. & Thieme, J. G. 1972 Outline of the geology of Zambia. *Geol. Mijnb.* **51**, 265–276.

Dunnet, D. 1969 A technique of finite strain analysis using elliptical particles. *Tectonophysics* **7**, 117–136.

Lightfoot, B. 1923 Interim report on the geology of part of the Darwin mineral belt. *S. Rhodesia geol. Surv. Short Rpt.* No. 15.

Lightfoot, B. & Tyndale-Biscoe, T. 1931 The geology of the country west of Mount Darwin. *Bull. geol. Surv. S. Rhod.* **10**.

Ramsay, J. G. 1967 *Folding and fracturing of rocks*. New York: McGraw-Hill.

Ramsay, J. G. & Wood, D. S. 1973 The geometric effects of volume change during deformation processes. *Tectonophysics* **16**, 263–277.

Talbot, C. J. 1967 Rock deformation at the eastern end of the Zambezi orogenic belt, Rhodesia. Unpublished Ph.D. thesis, University of Leeds.

Talbot, C. J. 1971 Thermal convection below the solidus in a mantled gneiss dome, Fungin Reserve, Rhodesia. *J. geol. Soc. Lond.* **127**, 377–410.

Vail, J. R. 1965 Progress report on regional studies of the Umkondo System and Fingoe Series, Central Africa. *9th Ann. Rep. res. Inst. afr. geol. Leeds*, 11–14.

Vail, J. R. 1966 Aspects of the stratigraphy and structure of the Umkondo System in the Manica belt of Southern Rhodesia and Mozambique, and an outline of the regional geology. *Trans. Geol. Soc. S. Africa* LXVII.

Wagner, P. A. 1913 A traverse through the northern portion of the Maza district of Southern Rhodesia into Portuguese territory. *Trans. geol. Soc. S. Afr.* XV, 124–139.

Wiles, J. W. 1961 The geology of the Miami Mica Field (Urungwe district). *Bull. geol. Surv. S. Rhod.* **51**.

Wiles, J. W. 1968 Some aspects of the metamorphism of the basement complex in the Sipolilo district. *Trans. geol. Soc. S. Afr. Annexure to* **71**, 79–85.

PHILOSOPHICAL TRANSACTIONS OF THE ROYAL SOCIETY A MATHEMATICAL, PHYSICAL & ENGINEERING SCIENCES

Workman, D. R. 1961 The geology of Mhavare-north-west Lomgundi district, Southern Rhodesia. Unpublished Ph.D. thesis, University of Leeds.
Worst, B. G. 1960 The Great Dyke of Southern Rhodesia. *Bull. geol. Surv. S. Rhodesia* 47.

Discussion

DR C. J. TALBOT (*Department of Geology, The University, Dundee, DD1 4HN*). Three different types of Pan-African belts have emerged so far in this conference. First there is the suturing type implying ocean closure in the southern part of the Arabian shield in Proterozoic times described by Greenwood and his co-workers. Then there are the ensialic orogenic segments, such as the Zambezi Belt, distinguishable into what Clifford (1967) called the geosynclinal facet (with a sedimentary cover which suffered the orogeny) and the vestigial facet consisting of reactivated continental rocks without a cover sequence. Dr Barr has taken strains determined in a vestigial facet (Rufunsa) and combined them with strains determined in a geosynclinal facet (Chimanda) and extrapolated them across the complete width of the belt. Having studied the strains in the easier of the two areas (Talbot 1973) – where the Umkondo metasediments record the effects of the Proterozoic orogeny only, I must congratulate Dr Barr on his optimism and success in quantifying the Proterozoic strains in the more difficult vestigial zone in Rufunsa in which earlier strains had to be considered.

Although the strains may be comparatively well known within the areas studied in detail however, the extrapolation across the less well known areas between and beyond is rather more ambitious and more open to question.

There are always likely to be obscured zones through which sutures representing the closed sites of former oceans may be drawn and there is no proof that such hidden structures do not exist in the generally ensialic Zambezi Belt. I would be happier, however, if at least one of the exposed candidates for such sutures could be rejected by future field geology. Thus a major east–west structural disconformity is visible on air photographs of the southern margin of the Mvuradhonna Mountains (north of Mount Darwin in the Rhodesian portion of the Zambezi Belt). A reconnaissance in 1964 suggested to me that this was a northerly dipping thrust separating the well differentiated Umkondo metasediments characteristic of the east end of the Zambezi Belt from a different sequence of turbidites which dip north before disappearing beneath the Karroo sediments at the fault bounding the Zambezi Valley.

This possible thrust aside, I must agree with Dr Barr's general thesis: that the large strains in the Zambezi Belt show little sign of adding up to a large Proterozoic shortening across the Belt. I chose the Chimanda area as a key to the Zambezi Belt after air photo interpretation of the whole of the northern edge of Rhodesia because it had a zone of simple linear air photo trends as well as the more characteristic and extensive zones of circular or nodal trends. Although north–south shortening appears to have occurred across the zone of linear trends early in the orogeny this was partially negated by subsequent crossfolding while elsewhere (Talbot 1973) basement domes developed in the zones of nodal trends.

References

Clifford, T. N. 1967 The Damaran episode in the Upper Proterozoic–Lower Palaeozoic structural history of southern Africa. *Spec. Pap. geol. Soc. Am.*, No. 92.
Talbot, C. J. 1973 The geology at the eastern end of the Zambezi Orogenic Belt, Rhodesia. *Trans. geol. Soc. S. Africa* **76**, 113–134.

PHILOSOPHICAL TRANSACTIONS OF THE ROYAL SOCIETY A MATHEMATICAL, PHYSICAL & ENGINEERING SCIENCES